

3.1 Bericht Teilprojekt 12

3.1.1 Thema / Title

Silizium-Nanokristallite in Matrizen und ihre Beziehung zur Extended Red Emission
Silicon nanocrystals in matrices and their relation to the Extended Red Emission

3.1.2 Berichtszeitraum / Reported period

1.02.2004 – 31.12.2006

3.1.3 Projektleiter / Principal investigator

Friedrich Huisken, Prof. Dr.
Max-Planck-Institut für Astronomie, Heidelberg, und
Institut für Festkörperphysik, Universität Jena

Wolfgang Witthuhn, Prof. Dr.
Institut für Festkörperphysik, Universität Jena

3.2 Zusammenfassung / Abstract

3.2.1 Wortlaut des Antrags / Abstract of the proposal

Gegenstand des Projekts ist die Präparation von Silizium-Nanokristalliten in verschiedenen Festkörpermatrizen sowie die Untersuchung ihrer optischen Eigenschaften im sichtbaren und nahen infraroten Spektralbereich. Die Arbeiten sollen Auskunft darüber geben, ob im Festkörper eingebettete Silizium-Kristallite als Träger der Extended Red Emission in Frage kommen. Zur Herstellung der Analogmaterialien sollen im wesentlichen zwei Verfahren Anwendung finden: (1) Implantation von Silizium-Ionen in Quarz- und Silikatträgern und (2) Laserverdampfung von pulverisiertem Si, SiO, SiO₂ und Silikaten mit einem Überschuß an Silizium. Die Ausbildung der Silizium-Nanokristallite erfolgt durch anschließendes Tempern bei 1200 °C. Zur optischen Charakterisierung gehört die Aufnahme von Photolumineszenzspektren nach Anregung mit der vierten Harmonischen eines Nd:YAG-Lasers sowie die Erfassung der Abklingzeiten. In einer weiteren Experimentreihe soll untersucht werden, inwieweit die Lumineszenz durch Ladungen auf der Oberfläche der Si-Nanoteilchen gequencht wird.

This project aims at preparing silicon nanocrystallites in various solid state matrices and investigating their optical properties in the visible and near infrared spectral regions. The studies will supply information on whether or not matrix-embedded silicon nanocrystallites are possible carriers for the Extended Red Emission. For the preparation of analogue materials, essentially two methods will be employed: (1) Implantation of silicon ions into quartz and silicate substrates, and (2) laser vaporization of Si, SiO, SiO₂ and silicate powders with an excess of silicon. The formation of silicon nanocrystallites is achieved by annealing at 1200 °C. Finally, the optical characterization is performed by recording photoluminescence (PL) spectra after excitation with the 4th-harmonic radiation of a Nd:YAG laser and studying the decay behavior of the PL. In another series of experiments, we will explore to what extent charges on the surface of the Si nanoparticles quench the luminescence.

3.2.2 Zusammenfassung des Berichts / Abstract of the report

Employing the accelerator facilities of the Institute of Solid State Physics of the University of Jena, we have implanted Si ions into quartz windows. By annealing the samples at temperatures around 1000 °C, silicon nanocrystals are formed within the SiO₂ matrix. Upon excitation with UV light, most samples reveal strong photoluminescence (PL) which is believed to result from quantum confinement. The optical properties of the matrix-embedded Si nanocrystals were studied as a function of the implantation conditions, the annealing parameters, and the temperature. The studies concentrated on the spectral and temporal behaviors (PL intensity vs. wavelength and PL intensity vs. time, respectively). In order to simulate matrix environments which resemble magnesium-rich silicates (forsterite and enstatite), we have also implanted magnesium ions at various fluences. It turned out that the PL originating from the silicon nanocrystals is severely quenched when the magnesium density is increased. Other elements (Ca, Na, and Ge) show the same trend. It is assumed that the quenching results from

the positive charge (constituting a defect) that remains in the nanocrystal while the electron is trapped by an foreign ion residing at the interface between the Si nanocrystal and the matrix. It is only for Er where we observe an energy transfer giving rise to an enhanced emission of the erbium ion at 1536 nm. As far as the astrophysical implication is concerned, it is concluded that Si nanocrystals are still promising candidates for the Extended Red Emission. They can be agglomerated to larger free-flying aggregates or they can be embedded in SiO₂ grains. In contrast, Si nanocrystals embedded in silicate grains cannot contribute to the emission due to the non-radiative recombination of the excitons at defects generated in the crystals upon the excitation.

3.3 Ausgangsfragen, neuester Stand der Forschung / Initial goals, current status of the field

Silicon nanocrystals are discussed as possible carriers of the Extended Red Emission (ERE), an astrophysical phenomenon observed in many stellar objects and clouds, and even in the Diffuse Interstellar Medium (Ledoux *et al.* 1998; Witt *et al.* 1998). Recently, our laboratory studies on oxygen-passivated silicon nanocrystals have shown that all ERE spectra known so far can be perfectly matched by laboratory spectra, suggesting that Si nanocrystals are responsible for this astrophysical luminescence phenomenon (Ledoux *et al.* 2001). However, more recent model calculations revealed that free-flying oxygen-passivated Si nanocrystals should give rise to an emission feature around 20 μm, which in fact is not observed in ERE regions (Li & Draine 2002). A possibility to satisfy this constraint is to assume that the Si nanocrystals are not individual free-flying nanoparticles, but instead agglomerated to clusters of nanoparticles or embedded in larger grains of some other material.

3.3.1 Initial Goals

To follow this idea, we have initiated a research program to study the photoluminescence (PL) of Si nanocrystals embedded in various solid matrices. The nanocrystals are generated by producing an excess concentration of silicon atoms in the respective material by ion implantation. Finally, the condensation of Si atoms to silicon nanoparticles and their crystallization is achieved by proper annealing at temperatures of 1000 °C and above (Cheylan & Elliman 1999).

As has been demonstrated by several authors (Garrido *et al.* 2004, Takeoka *et al.* 2000, Kahler & Hofmeister 2001), Si nanocrystals embedded in SiO₂ reveal strong photoluminescence (PL) the origin of which is still controversially discussed (quantum confinement or interface defects). It was planned to employ various implantation and annealing conditions to produce light-emitting samples and to study the spectral and temporal behaviors of this light emission as a function of the synthesis parameters, post-treatment conditions, and temperature. In a second step, it was planned to dope the samples with Mg²⁺ ions with increasing concentration to simulate the conditions prevailing in magnesium-rich silicate grains (forsterite and enstatite) and to study the effect on the PL of the Si nanocrystals. Other dopants (Ca²⁺, Na⁺, Ge⁺, Er³⁺ *etc.*) were considered as well. The investigations were aimed at contributing to the question whether Si nanocrystals embedded in Si-based grains were potential candidates for the Extended Red Emission.

3.3.2 Current status of the field

The issue of Si nanocrystals being responsible for the ERE was strongly supported by Witt *et al.* (1998) and Smith & Witt (2002). During the course of the present project, Witt and co-workers performed new observations in the Red Rectangle which is famous for its red luminescence. They discovered a new kind of luminescence in the blue (centered at 375 nm) that they associated with the emission from small neutral polycyclic aromatic hydrocarbons (PAHs) consisting of three to four aromatic rings such as anthracene and pyrene (Vijh *et al.* 2004). Following this study, Mulas *et al.* (2006) computed the phosphorescence emission fluxes for a few candidates and found that only anthracene appears compatible with the observations. On the other hand, Nayfeh *et al.* (2005) bring Si nanocrystals into play again. They suggest that ultrasmall Si nanoparticles with diameters of 1 nm could be the origin of the blue luminescence as well.

Very recent observations of NGC 7023 with the Hubble Space Telescope provided new constraints for the character of the ERE carrier (Witt *et al.* 2006). The authors suggest that the ERE carriers are produced by far-UV photons with energies in excess of 10.5 eV, probably through photoionization or photodissociation of an existing precursor and that the red luminescence results from the excitation of these carriers by near-UV/optical photons. Candidates compatible with this pictures would be doubly ionized PAH molecules (PAH dications). Unfortunately, no laboratory data is available for such exotic species so that the suggestion is difficult to prove. Summarizing the most recent results on the red and blue emissions in the Red Rectangle, it appears that PAHs and Si nanocrystals are at present the most widely discussed carrier candidates.

3.4 Angewandte Methoden / Experimental methods

3.4.1 Ion implantation

In the present study, we used two different kinds of substrates into which the Si ions were implanted: (1) 0.2-mm-thick quartz plates (Heraeus Suprasil 1) and (2) thermally oxidized Si wafers covered with a 300-nm-thick SiO₂ layer (Crystec). The ion implantation was performed employing the ion implanter ROMEO of the Institute of Solid State Physics, Jena. As ion energy, we chose 100 or 105 keV while the ion fluence was varied between 0.5×10^{17} and 2×10^{17} Si ions per cm². According to SRIM calculations carried out for this energy, a distribution of penetration depths with a maximum at 150 nm and a full width at half maximum of 100 nm was determined.

3.4.2 Annealing

The as-implanted samples were annealed for one hour at temperatures between 900 and 1100 °C. In all experiments discussed here, the annealing temperature was 1100 °C. To avoid any further oxidation, the annealing was carried in an atmosphere of nitrogen. When the samples are heated to such temperatures, the implanted Si ions diffuse within the matrix to nucleate and grow to clusters and small nanoparticles. While the melting point of bulk silicon is 1414 °C, Si clusters are expected to be in the liquid state. Upon slow cooling, the Si clusters crystallize to form defect-free Si nanocrystals concentrated in a layer 150 nm below the surface through which the ions were implanted.

3.4.3 Spectral and temporal photoluminescence studies

In contrast to bulk silicon, Si nanocrystals do emit light when they are excited by UV photons. This effect is attributed to the relaxation of the selection rules as a result of quantum confinement. The photoluminescence (PL) of the matrix-embedded Si nanocrystals has been studied in both the spectral and temporal domain using a dedicated self-made PL spectrometer. As excitation source, we used the fourth harmonic ($\lambda = 266$ nm) of a pulsed Nd:YAG laser (Continuum Minilite II, pulse width: 6 ns, maximum energy at 266 nm: 12 mJ per pulse). In order to avoid saturation effects, the UV laser beam is always attenuated to energy values below 15 μ J/pulse. Finally it is focused on the sample to a spot size of 1 mm diameter. The PL emanating from the excited spot is collected by a lens with a focal length of 70 cm and imaged by another lens ($f = 30$ cm) on the 3-mm-wide entrance slit of a 30-cm monochromator (McPherson, model 218-VUV-Vis-IR). The dispersed PL is detected by a *l*-N₂-cooled photomultiplier (Hamamatsu, model R5509-72) with high detection efficiency in the near-IR (up to 1.7 μ m). PL spectra are recorded by step-scanning the monochromator and collecting the signal in a computer-controlled gated integrator incorporated into a CAMAC module. The decay of the luminescence upon excitation is measured with a digital oscilloscope (Tektronix TDS320). During the decay measurement, the monochromator is parked at a distinct wavelength.

When we want to study the temperature dependence of the photoluminescence the sample is mounted on the cold finger of a closed-cycle helium cryostat (ADP DE-204-SL). The lowest temperature achieved is 6.5 K.

3.4.5 Implantation of foreign ions

After having characterized the samples regarding their optical properties, some of them were exposed to a beam of foreign ions (Mg, Ca, Na, Er). The energy was chosen such that the mean penetration depth was again 150 nm. To heal the defects originating from the second implantation, the samples were annealed at a temperature of 900 °C (post-annealing). The following characterization of the optical properties (PL frequency dependence and excited state lifetime measurements) yields valuable information on the interaction between the Si nanocrystals and the foreign atoms or, more specifically, between the exciton produced upon UV excitation and the foreign atoms in the surrounding SiO₂ matrix.

3.5 Ergebnisse und ihre Bedeutung / Results and their importance

3.5.1 Synthesis of nc-Si embedded in SiO₂ by ion implantation

Nanocrystalline silicon centers (nc-Si) are synthesized by the nucleation of excess silicon supplied by ion implantation in the SiO₂ matrix and by subsequent annealing generally performed at temperatures between 500 and 1200 °C. As shown by Garrido *et al.* (2004), the size of nc-Si depends on the concentration of the excess silicon and the duration of the annealing, but also on the annealing temperature (Cheylan *et al.* 2000). Ion irradiation generates defects in quartz that exhibits parasite luminescence around 650 nm, caused by non-bridging oxygen centers in the SiO₂ matrix. Cheylan *et al.* (2000) clearly demonstrated that an annealing treatment quenches this effect and, on the contrary, enhances the PL originating from the Si nanocrystals.

Figure 1 shows the PL spectra as a function of the excess of silicon for an annealing temperature of 1100 °C. It is seen that the PL maximum shifts to longer wavelengths (smaller energies) when the ion fluence is

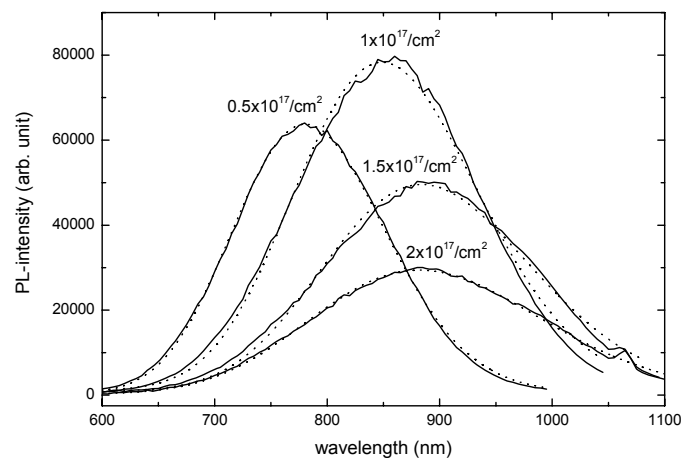


Fig. 1: PL spectra of quartz windows into which silicon was implanted at fluences of 0.5, 1, 1.5, and 2×10^{17} atoms per cm^2 . Annealing at 1100 °C in N₂ was performed for one hour. The peak positions and halfwidths were evaluated by fitting log-normal distributions (dotted lines) to the data.

increased. This can be understood in view of the quantum confinement effect. According to the quantum confinement model, a PL maximum at larger (shorter) wavelength correlates with a larger (smaller) average size of the Si nanocrystals.

For large fluences, the red shift resulting from a further increase of the fluence becomes less pronounced. This is consistent with the asymptotic Ostwald ripening growth model of nc-Si (Garrido *et al.* 2004) where, for one annealing condition (temperature and duration), the size of nc-Si increases with the excess of silicon but to a lower extent.

Figure 1 also shows an increase of the PL intensity when the maximum position moves from 780 to 860 nm and a subsequent decrease for the spectra peaking above 860 nm. This is consistent with the PL yield measured by Ledoux *et al.* (2002) for free nc-Si covered by a SiO₂ layer produced by laser pyrolysis of silane. In their study, the maximum yield was found for an average size of 3.8 nm which corresponds to a PL emission wavelength of 840 nm for the same nc-Si diameter embedded in quartz. This behavior of the PL intensity can be explained by the concerted action of two effects: the decreasing PL efficiency as a result of reduced quantum confinement and the increased probability of encountering a defect in the nc-Si.

3.5.2 Temporal behavior of the photoluminescence from nc-Si

The multi-exponential behavior of the decay curves of an ensemble of nc-Si was observed before by other researchers (Linnros *et al.* 1997). The decay curves are usually fitted by a Kohlrausch function $I(t) = I_0 \exp[-(t/\tau)^\beta]$ where τ is the lifetime and β the dispersion factor. Analogous properties have been observed for the luminescence of CdSe quantum dots. Schlegel *et al.* (2002) and Fischer *et al.* (2003) showed that the multi-

exponential feature is intrinsic of one single quantum dot. They noticed that the decay lifetimes correlated strongly with the luminescence intensity fluctuations where a high fluorescence yield is associated with a long fluorescence lifetime. In particular, at the highest fluorescence intensity, the decay curves were found to approach a single-exponential behavior.

In the main frame of Fig. 2, we have plotted the decay curves of the nc-Si PL as measured on a sample produced with an ion fluence of $1 \times 10^{17} \text{ cm}^{-2}$. From left to right, the emission wavelength varies from 675 to 1000 nm in steps of 25 nm, *i.e.* the lifetime increases as the emission wavelength becomes larger. The decay rates were evaluated by fitting

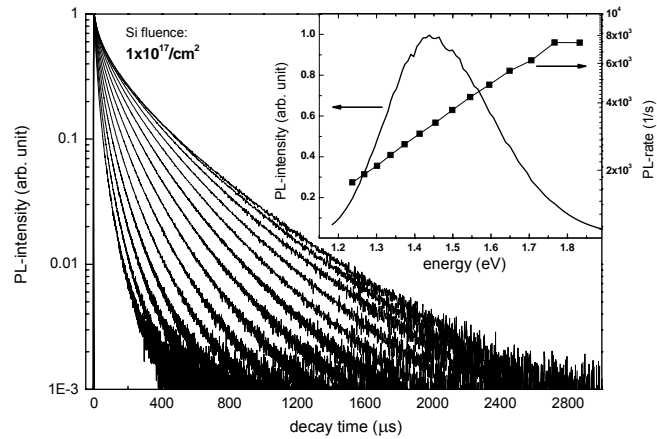


Fig. 2: PL decay curves of silicon quantum dots embedded in quartz recorded from 675 nm (left curve) to 1 μm (right curve) with a step of 25 nm. The inset shows the PL spectrum of the respective sample as well as the decay rates as a function of emission energy.

log-normal decay rate distributions to the measured data using the maximum entropy method of data analysis (Delerue *et al.* 2006). Log-normal rate distributions were also employed to fit the decay curves of CdSe nanocrystals, but with another method (Van Driel 2006). However, it must be underlined that there is by no means a unique solution and that the decay curves can be fitted by different distributions of rates.

In the inset of Fig. 2, it is seen that the decay rate increases exponentially with the emission energy. An exponential increase following an $\exp(-E/E^*)$ law, where E is the photon energy and the parameter E^* varies between 0.2 and 0.4 eV, has been observed by several authors. Here we found $E^* = 0.35$ eV which is similar to the 0.25 and 0.31 eV values, respectively, found by Huisken *et al.* (2002) and Delerue *et al.* (2006). This functional form has always been observed for quantum-confined nanostructures but its physical background still remains unexplained.

3.5.3 Temperature dependence of the PL of nc-Si embedded in SiO_2

Figure 3 shows PL spectra measured at 6.5, 12.5, 25, 50, 100, 200, and 300K in vacuum. As the temperature falls, the PL integrated intensity

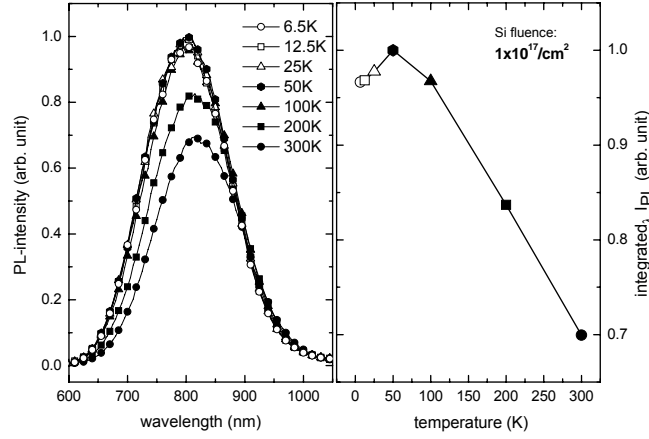


Fig. 3: Temperature dependence of PL emission spectra of nc-Si embedded in SiO₂.

increases and reaches a maximum at 50 K. At the same time, the spectra become broader and shift slightly to the blue.

This effect was also previously reported (Brongersma *et al.* 2000) and explained by a model introduced by Calcott *et al.* (1993) initially for porous silicon. In this model, the localized excitonic levels are split by an energy Δ , due to the exchange interaction between the electron and the hole. The lower level corresponds to a triplet state which has a radiative rate R_T . The upper level corresponds to a singlet state with a radiative rate R_S . The temperature dependence of the total radiative decay rate, R_R , can be evaluated by assuming thermal equilibrium between the two levels. Thus the rate becomes $R_R = [3R_T + R_S \exp(-\Delta/kT)]/[3 + \exp(-\Delta/kT)]$.

At low temperature, only the triplet state is occupied and the radiative decay rate is rather small. When the temperature is raised, the population of the upper level, which is characterized by a faster decay, becomes more important. The PL quantum yield η_{PL} is a function of the radiative and non-radiative rates and can be written as $\eta_{PL} = R_R/(R_R + R_{NR})$. This explains why the PL intensity increases when the temperature is raised from lower values to 75 K, typically reported. The decrease of the PL intensity for temperatures above 75 K can be explained by the fact that non-radiative processes between nc-Si and the SiO₂ matrix become more effective.

3.5.4 Quenching of the photoluminescence by magnesium doping

Quartz windows containing luminescent nc-Si were doped with magnesium by ion implantation with fluences from 3.2×10^{12} to 3.2×10^{14} cm⁻² followed by an annealing at 900 °C (post-annealing) in an oxygen-free atmosphere for one hour. The implantation energy was chosen such that the magnesium implantation depth coincides with the nc-Si layer location in the quartz window. Directly after implantation, no PL from nc-Si, or at best a very weak PL for the lowest doping ion concentration, was observed. This seems to prove that all or most of the nc-Si were irretrievably damaged as a result of the ion irradiation. The PL was partially recovered after the post-annealing treatment depending on the doping ion fluence, as illustrated in Fig. 4.

The figure illustrates that, as the magnesium fluence increases, the nc-Si PL intensity is more and more quenched. It was also noticed that the luminescence can be completely turned off with Mg fluences higher than 1×10^{15} cm⁻². This could be expected by extrapolating the curve in the right panel that describes the PL quenching as a function of the magnesium fluence. The quenching effect is associated with a red shift, which continually increases with the concentration of the dopant. Such doping

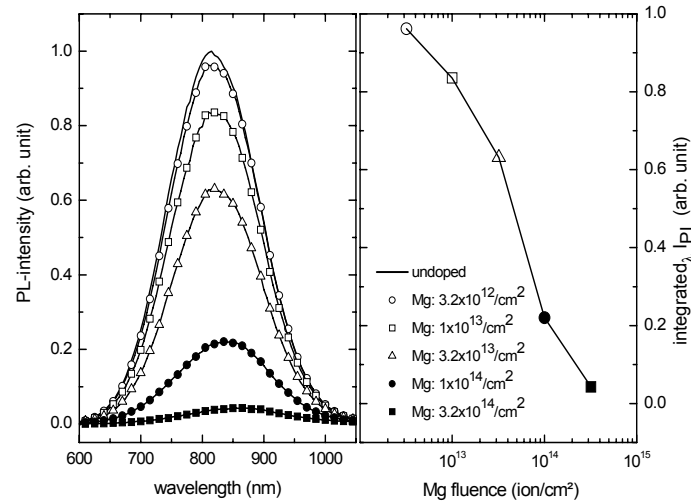


Fig. 4: Effect of Mg doping on the photoluminescence of nc-Si embedded in SiO₂. Quartz windows containing luminescent nc-Si synthesized by ion implantation with a Si fluence of $1 \times 10^{17} \text{ cm}^{-2}$ and a subsequent annealing at 1100 °C were implanted with Mg at different fluences and annealed at 900 °C

effects were also observed by Fujii *et al.* (2003) for nc-Si embedded in SiO₂ and boron as dopant. The samples were produced by co-sputtering using similar dopant concentrations. They could quench the PL down to 3% of the original value with a corresponding red shift of 70 nm. This is similar to our result yielding a maximum red shift of 42 nm in conjunction with a quenching of 4%.

The quenching of the PL can be explained by an interaction between the electron of the exciton with the positively charged Mg which we assume to reside outside the crystalline Si core. The electron is trapped and the hole remaining in the nanocrystal acts as a defect causing the non-radiative recombination of newly formed excitons. Smaller Si nanocrystals are expected to be more sensitive to this effect because the electron can be extracted more easily from the core. As smaller nanocrystals emit at shorter wavelengths, their enhanced quenching results in a red shift of the ensemble spectrum.

It seems that the order of the implantation phases – silicon implantation and magnesium implantation – does not play any role on the quenching of nc-Si PL. This was proved by another experiment, where Si nanocrystals were synthesized in previously doped quartz plates with the same concentrations and where no significant difference was observed. As a result, the PL quenching and the red shift should not be discussed in

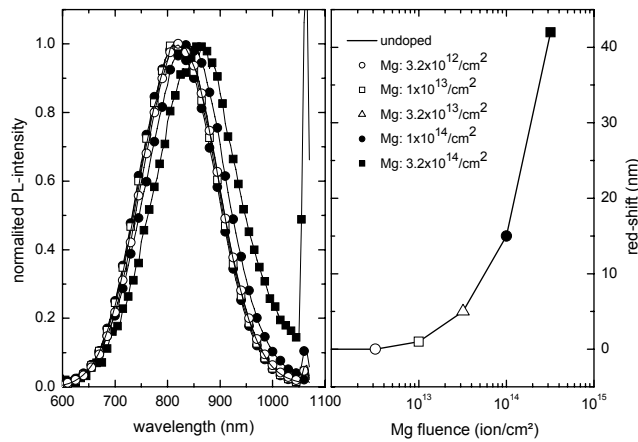


Fig. 5: Effect of magnesium doping on the maximum position of the PL of nc-Si synthesized by ion implantation (left: normalized spectra, right: red shift as a function of Mg fluence).

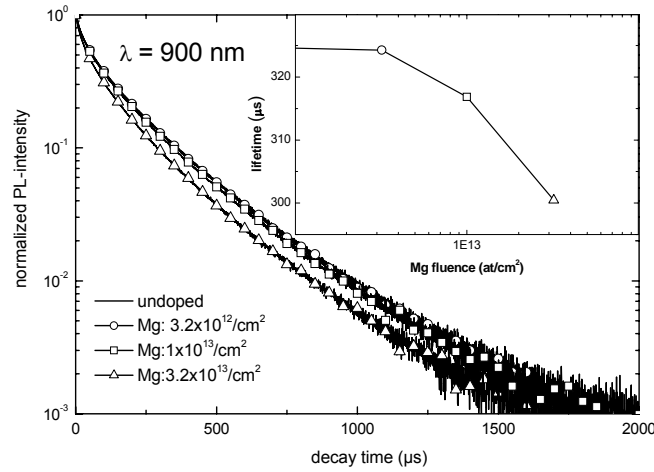


Fig. 6: Effect of magnesium doping on the PL decay of nc-Si synthesized by ion implantation.

terms of ion irradiation effects but in terms of doping and concentration effects.

PL measurements for doped and undoped nc-Si were performed from low temperatures (starting at 6.5 K) to room temperature. They showed that the relative quenching and the inherent red shift between doped and undoped nc-Si samples are independent of the temperature.

In the time domain, the registration of decay curves was performed at several wavelength positions of the PL spectra for undoped and doped samples. A shortening of the decay lifetime (increase of the decay rate) with the doping fluence was observed, as illustrated in the Fig. 6 for a wavelength position of 900 nm. The increase of the decay rate was independent of the emission energy of the PL spectra, and can thus not explain the small red shift observed in the frequency (or wavelength) domain. Such PL shortening behavior was also observed by other researchers for samples doped with B, P (Fujii *et al.* 2003), Au (Tchebotareva *et al.* 2005) and Er (Franzò *et al.* 2000), and were explained by an increase of the non-radiative rates caused by defects due to the presence of dopant ions.

3.5.5 Photoluminescence from erbium coupled with nc-Si in SiO₂

The enhancement of erbium emission coupled with nc-Si has already been studied by other researchers (Franzò *et al.* 2000, Kik *et al.* 2000) and is usually explained as follows. The Si nanoparticles serve as antenna for the erbium ions as they absorb in a broad frequency range as long as the photon energy is larger than the band gap. In the present system, due to the long lifetime of the nc-Si, the excitation energy (corresponding to the band gap) is transferred to the Er ions enabling them to emit at 1536 nm. The attractive feature of this mechanism is the possibility to build amplifiers for the 1536 nm radiation of erbium. Because of this interest, the PL of systems containing nc-Si doped with Er is well documented in the literature. Therefore, we found it interesting to study this interaction and to compare the measurements with our results obtained for other dopants (*e.g.* nc-Si doped with magnesium).

Samples were prepared as described in the preceding section by implanting erbium ions with fluences from 3.2×10^{13} to 3.2×10^{15} cm⁻². The left part of Fig. 7 displays the quenching effect caused by Er doping on the PL spectra of nc-Si when the Er implantation fluence increases, while the right part shows the situation in the wavelength range around 1525 nm where Er³⁺ has an emission band (${}^4I_{13/2} \rightarrow {}^4I_{15/2}$ at 1.536 μm). The emission of erbium first increases with the concentration up to a fluence of 3.2×10^{14} cm⁻² and decreases for higher fluences. This can be

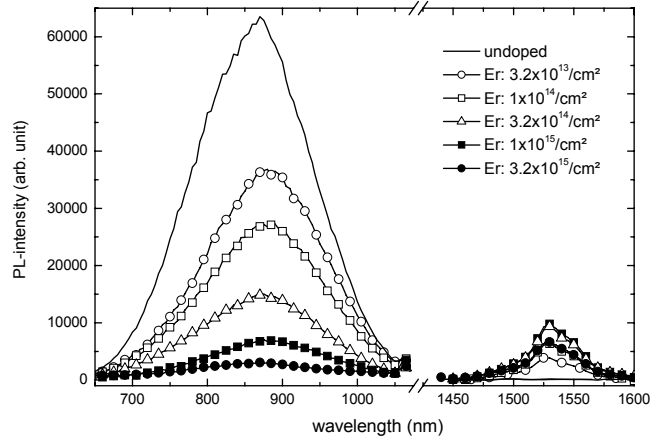


Fig. 7: Photoluminescence from nc-Si and erbium for samples produced with Er fluences between 3.2×10^{13} and $3.2 \times 10^{15} \text{ cm}^{-2}$.

ascribed to the fact that, as the Er concentration is increased, the number of Er emission centers increases as well. However, when the concentration of damaged nc-Si becomes too important, the exciton concentration available for Er excitation is consequently reduced, resulting in a decrease of the erbium emission.

3.5.6 Other dopants

Similar experiments were carried out with other dopants such as calcium, sodium, and germanium. The effects on the photoluminescence of nc-Si – quenching of PL, shortening of decay lifetimes, and slight red shift – were very similar to those described for magnesium. The results are summarized in Fig. 8 where, for various dopants, the quenching of the nc-Si is plotted as a function of the relative concentration of the foreign atoms ($n_{\text{atom}}/n_{\text{nc-Si}}$).

The concentrations of foreign atoms in the samples investigated in the present study are much lower than those expected in silicate grains. Other experiments, not described here, revealed that, for even higher concentrations, the PL of embedded Si nanocrystals is totally quenched. Only some weak parasite luminescence at lower emission wavelengths, resulting from the presence of defects in the SiO_2 matrix could be detected.

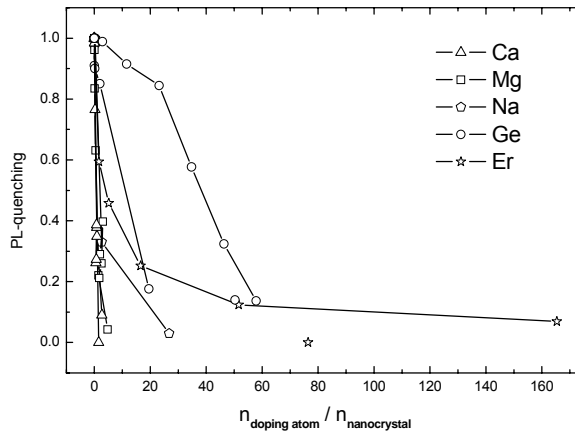


Fig. 8: Quenching of the photoluminescence of nc-Si plotted as a function of the number of foreign atoms per Si quantum dot. Here we have also included our results on calcium, sodium, and germanium which are not discussed in this report.

But this PL is not compatible with astrophysical observations. In summary, the present studies show that silicon nanocrystals embedded in silicate grains cannot account for the Extended Red Emission while Si nanocrystals in SiO_2 grains would still be good candidates together with agglomerated oxidized nc-Si (clusters of Si nanoparticles).

3.5.7 Comparison with other experiments

In Fig. 9, we summarize the results of the PL of silicon nanocrystals as a function of particle size as obtained by various authors using various methods (laser pyrolysis, ion implantation, co-sputtering, reactive evaporation of SiO, and PECVD). The solid line corresponds to the theoretical tight-binding study of Delerue *et al.* (1993) which is considered to be the most accurate computation. This curve is represented by an inverse

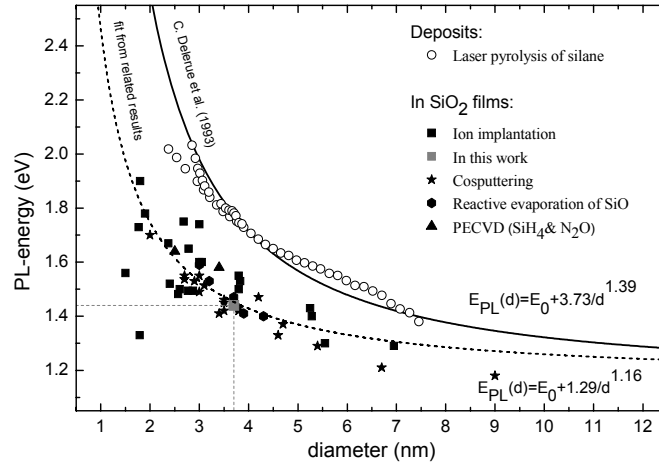


Fig. 9: Maximum positions of the PL curves, in terms of energy, as a function of the diameter of the crystalline core as obtained in various experiments. The open symbols correspond to laser pyrolysis experiments where the nanocrystals were produced as free particles in the gas phase (Ledoux *et al.* 2002). The solid symbols refer to Si nanocrystals in bulk SiO₂ or thin films (ion implantation: Guha *et al.* 2000, Garrido *et al.* 2000, Garrido *et al.* 2004, Hryciw *et al.* 2004, Sias *et al.* 2005, Franzò *et al.* 2001, and this work; co-sputtering: Fujii *et al.* 1998, Kanzawa *et al.* 1996, Mimura *et al.* 1999, Takeoka *et al.* 2000, Conibeer *et al.* 2006; reactive evaporation of SiO: Kahler and Hofmeister 2001; PECVD: Inokuma *et al.* 1997).

power law $E_{PL}(d) = E_0 + 3.73 d^{-1.39}$, where E_0 is the band gap of bulk silicon. It is seen that only the experimental data obtained for free oxygen-passivated Si quantum dots (Ledoux *et al.* 2002) comply with the theory. The other data points, corresponding to other synthesis methods, reveal smaller band gaps at a given diameter or smaller diameters at a given energy. For identical emission energies of 1.9 eV and 1.5 eV, silicon nanocrystals in a quartz matrix are, respectively, 49% and 43% smaller than free Si nanoparticles covered by a thin SiO₂ layer. The latter data points are best fitted by the power law $E_{PL}(d) = E_0 + 1.29 d^{-1.16}$.

From one of our samples discussed in the present report (having its PL maximum at $E = 1.44$ eV), we were recently able to obtain a HRTEM image and to determine the average size of the nanocrystals present in the sample ($d = 3.7$ nm). This data point agrees nicely with the other values obtained from ion-implanted samples.

The main difference between laser pyrolysis Si nanoparticles and the other Si nanocrystals is that the former nanoparticles were fully relaxed in the expansion of a supersonic helium jet before they were deposited on a substrate and subjected to a gentle oxidation. They are considered to be stress-free. In contrast, the nanocrystals synthesized by other methods are embedded in thin films or bulk SiO₂ matrices. It could be that they are subject to significant stress and that this is the reason for their different PL behavior. It is also possible that the PL in these systems is not of quantum-confined origin but defect-related as a result of the interaction between the exciton produced in the Si nanocrystal and the environment (matrix, film, or interface). The enhancement of the PL of erbium ions and the quenching of nc-Si PL by foreign ions supports the idea that there is a strong interaction between the Si nanocrystals and the surrounding.

3.6 Zusammenfassung und Ausblick / Summary and future

Within the present project, we have studied the photoluminescence properties of silicon nanocrystals embedded in SiO₂ matrices. The samples were prepared by Si ion implantation followed by an annealing treatment at 1100 °C. It is found that the silicon atoms condense to clusters and nanoparticles in the matrix

giving rise to a strong photoluminescence response upon excitation with UV photons. Such systems can be considered as analog materials for astrophysical dust grains (SiO₂ grains containing Si nanocrystals). Comparing the results with those obtained earlier on free Si nanocrystals, which led to the proposal that Si nanocrystals could be the carriers of the Extended Red Emission (ERE), it is found that the PL of a Si nanocrystal of specific size is shifted to longer wavelength or smaller energy. As a result, if the ERE observations are to be explained by Si nanocrystals embedded in SiO₂ grains, the size regime (2.5 – 6.5 nm) postulated for free nanocrystals must be shifted to (1.5 – 4 nm). Unfortunately, it was not possible to determine the quantum efficiency of the PL of matrix-embedded nc-Si because the size distribution of the nanocrystals is not known with sufficient accuracy. Therefore, it is difficult to obtain quantitative information on the PL strength which would be required to discuss embedded Si nanocrystals in context with the ERE issue.

In order to simulate the situation encountered in magnesium-rich silicate grains, we have implanted Mg ions (and other ions such as Na, Ca, Ge, and Er) with various fluences into the samples containing the luminescent Si nanocrystals. It is found that doping with foreign ions significantly quenches the PL of the Si nanocrystals. In the case of erbium implantation, we could show (together with other researchers) that the excitation energy is efficiently transferred from the Si nanocrystals to the erbium ions. This proves that there is considerable interaction between the crystalline Si cores and the surrounding, raising the question whether this is consistent with a purely quantum-confined origin of the photoluminescence. As far as the astrophysical issue of the ERE is concerned, it is clear that silicate grains with silicon-rich cores cannot be efficient light emitters. Therefore, silicates can be discarded as candidates for ERE carriers.

Acknowledgments

This work was supported by a cooperation between the Max-Planck-Institut für Astronomie and the Friedrich-Schiller-Universität Jena as well as by the Deutsche Forschungsgemeinschaft in the frame of the Forschergruppe *Laborastrophysik*.

3.7 Literatur / References

- Brongserma, M.L., Kik, P.G., Polman, A., Min, K.S., Atwater, A.: *Size-dependent electron-hole exchange interaction in Si nanocrystals*, Appl. Phys. Lett. **76** (2000) 351.
- Calcott, P.D.J., Nash, K.J., Canham, L.T., Kane, M.J., Brumhead, D.: *Spectroscopic identification of the luminescence mechanism of highly porous silicon*, J. Lumin. **57** (1993) 257.
- Carrada, M., Wellner, A., Paillard, V., Bonafos, C., Coffin, H., Claverie, A.: *Photoluminescence of Si nanocrystal memory devices obtained by ion beam synthesis*, Appl. Phys. Lett. **87** (2005) 251911.
- Cheyilan, S., Langford, N., Elliman: *The effect of ion-irradiation and annealing on the luminescence of Si nanocrystals in SiO₂*, Nucl. Instr. And Method. In Phys. Res. B **166-167** (2000) 851-856.
- Conibeer, G., Green, M., Corkish, R., Cho, Y., Cho, E.C., Jiang, C. W., Fangsuwannarak, T., Pink, E., Huang, Y., Puzzer, T., Trupke, T., Richards, B., Shalav, A., Lin, K.L.: *Silicon nanostructures for third generation photovoltaic solar cells*, Thin Solid Films **511-512** (2006) 654.
- Delerue, C., Allan, G., Lannoo, M.: *Theoretical aspects of the luminescence of porous silicon*, Phys. Rev. B **48** (1993) 11024.
- Delerue, C., Allan, G., Reynaud, C., Guillois, O., Ledoux, G., Huysken, F.: *Multiexponential photoluminescence decay in indirect-gap semiconductor nanocrystals*, Phys. Rev. B **73** (2006) 235318.
- Ding, L., Chen, T.P., Liu, Y., Ng, C.Y., Liu, Y.C., Fung, S.: *Thermal annealing effect on the band gap and dielectric functions of silicon nanocrystals embedded in SiO₂ matrix*, Appl. Phys. Lett. **87** (2005) 121903.
- Fisher, B.R., Eisler, H.G., Scott, N.E., Bawendi, M.G.: *Emission Intensity Dependence and Single-Exponential Behaviour In Single Colloidal Quantum Dot Fluorescence Lifetimes*, J. Phys. Chem. B **108** (2004) 143-148.
- Franzò, G., Pacifici, D., Vinciguerra, V., Priolo, F., Iacoma, F.: *Er³⁺ ions-Si nanocrystals interactions and their effects on the luminescence properties*, Appl. Phys. Lett. **76** (2000) 2167.
- Franzò, G., Moreira, E.C., Pacifici, D., Priolo, F., Iacona, F., Spinella, C.: *Ion beam synthesis of undoped and Er-doped Si nanocrystals*, Nucl. Instr. and Meth. In Phys. Res. B **175-177** (2001) 140.
- Fujii, M., Toshikiyo, K., Takase, Y., Yamaguchi, Y., Hayashi, S.: *Below bulk-band-gap photoluminescence at room temperature from heavily P- and B-doped Si nanocrystals*, J. Appl. Phys. **94** (2003) 1990.
- Fujii, M., Yoshida, M., Hayashiand, S., Yamamoto, K.: *Photoluminescence from SiO₂ films containing Si nanocrystals and Er: Effects of nanocrystalline size on the photoluminescence efficiency of Er³⁺*, J. Appl. Phys. **84** (1998) 4526.
- Garrido, B., Lopez, M., Gonzalez, O., Perez-Rodriguez, A., Morante, J. R., Bonafos, C.: *Correlation between structural and optical properties of Si nanocrystals embedded in SiO₂: The mechanism of visible light emission*, App. Phys. Lett. **77** (2000) 3143.
- Garrido, B., Lopez, M., Perez-Rodriguez, A., Garcia, C., Pellegrino, P., Ferre, R., Moreno, J.A., Morante, J.R., Bonazos, C., Carrada, M., Claverie, A., de la Torre, J., Souifiet, A.: *Optical and electrical properties of Si-nanocrystals ion beam synthesized in SiO₂*, Nucl. Instr. and Meth. In Phys. Res. B **216** (2004) 213.

- Guha, S., Qadri, S. B., Musket, R. G., Wall, M. A., Shimizu-Iwayama, T.: *Characterization of Si nanocrystals grown by annealing SiO₂ films with uniform concentrations of implanted Si*, J. Appl. Phys. **88** (2000) 3954.
- Hryciw, A., Meldrum, A., Buchanan, K.S., White, C.W.: *Effects of particle size and excitation spectrum on the photoluminescence of silicon nanocrystals formed by ion implantation*, Nucl. Instr. and Meth. in Phys. Res. B **222** (2004) 469.
- Huisken, F., Ledoux, G., Guillois, O., Reynaud, C.: *Light-Emitting Silicon Nanocrystals from Laser Pyrolysis*, Adv. Mater. **14** (2002) 1861.
- Inokuma, T., Wakayama, Y., Muramoto, T., Aoki, R., Kurata, Y., Hasegawa, S.: *Optical properties of Si clusters and Si nanocrystallites in high-temperature annealed SiO_x films*, J. Appl. Phys. **83** (1998) 2228.
- Kahler, U., Hofmeister, H.: *Visible light emission from Si nanocrystalline composites via reactive evaporation of SiO*, Optical Materials **17** (2001) 83.
- Kanzawa, Y., Kageyama, T., Takeoka, S., Fujii, M., Hayashi, S., Yamamoto, K.: *Size-dependent near-infrared photoluminescence spectra of si nanocrystals embedded in SiO₂ matrices*, Solid State Communication **102** (1997) 533.
- Kik, P.G., Brongersma, M.L., Polman, A.: *Strong exciton-erbium coupling in Si nanocrystal-doped SiO₂*, Appl. Phys. Lett. **76** (2000) 2325.
- Kik, P.G., Polman, A.: *Exciton-erbium energy transfer in si nanocrystal-doped SiO₂*, Materials Science and Engineering B **81** (2001) 3-8.
- Ledoux, G., Guillois, O., Huisken, F., Kohn, B., Porterat, D., Reynaud, C.: *Crystalline silicon nanoparticles as carriers for the Extended Red Emission*, Astron. Astrophys. **377** (2001) 707.
- Ledoux, G., Gong, J., Huisken, F., Guillois, O., Reynaud, C.: *Photoluminescence of size separated silicon nanocrystals*, Appl. Phys. Lett. **80** (2002) 4834.
- Linnros, J., Galeckas, A., Lalic, N., Grivickas, V.: *Time-resolved photoluminescence characterisation of nm-sized silicon crystallites in SiO₂*, Thin Solid Films **297** (1997) 167-170.
- Mimura, A., Fujii, M., Hayashia, S., Yamamotoa, K.: *Quenching of photoluminescence from Si nanocrystals caused by Boron doping*, Solid State Communications **109** (1999) 561.
- Mulas, G., Malloci, G., Joblin, C., Toublanc, D.: *Estimated IR and phosphorescence emission fluxes for specific polycyclic aromatic hydrocarbons in the Red Rectangle*, A&A **446** (2006) 537-549.
- Nayfeh, M.H., Shadia, R.H., Rao, S.: *Crystalline Si nanoparticles as carriers of the blue luminescence in the Red Rectangle nebula*, Astrophys. J. **621** (2005) L121-L124.
- Schlegel, G., Bohnenberger, J., Potapova, I., Mews, A.: *Fluorescence Decay Time of Single Semiconductor Nanocrystals*, Phys. Rev. Lett. **88** (2002) 137401-1.
- Smith, T.L., Witt, A.N.: *The photophysics of the carrier of the Extended Red Emission*, Astrophys. J. **565** (2002) 304-318.
- Sias, U. S., Amaral, L., Behar, M., Boudinov, H., Moreira, E.C., Ribeiro, E.: *Photoluminescence behavior of Si nanocrystals as a function of the implantation temperature and excitation power density*, J. Appl. Phys. **98** (2005) 034312.
- Takeoka, S., Fujii, M., Hayashi, S.: *Size-dependent photoluminescence from surface-oxidized Si nanocrystals in a weak confinement regime*, Phys. Rev. B **62** (2000) 16820.
- Tchebotareva, A.L., Michiel, J.A., Biteen, J.S., Atwater, H.A., Polman, A.: *Quenching of Si nanocrystal photoluminescence by doping with gold or phosphorous*, J. Lumim. **114** (2005) 137-144.
- Van Driel, A. F.: *PhD thesis: Light Sources in Semiconductor Photonic Materials*, Universiteit Utrecht (2006).
- Vijh, U.P., Witt, A.N., Gordon, K.D.: *Discovery of blue luminescence in the Red Rectangle: Possible fluorescence from neutral polycyclic aromatic hydrocarbon molecules?*, Astrophys. J. **606** (2004) L65-L68.
- Witt, A.N., Gordon, K.D., Furton, D.G.: *Silicon Nanoparticles: Source of Extended Red Emission?*, Astrophys. J. **501** (1998) L111-L115.
- Witt, A.N., Gordon, K.D., Vijh, U.P., Sell, P.H., Smith, T.L., Xie, R.-H.: *The excitation of Extended Red Emission: New constraints on its carrier from Hubble space telescope observations of NGC 7023*, Astrophys. J. **636** (2006) 303-315.